International Scholarly Research Network
ISRN Communications and Networking
Volume 2011, Article ID 701670, 14 pages
doi:10.5402/2011/701670

Research Article

Turbo-Coded MC-CDMA Communication Link over Strong Turbulence Fading Limited FSO Channel with Receiver Space Diversity

MD. Zoheb Hassan, Tanveer Ahmed Bhuiyan, S. M. Shahrear Tanzil, and S. P. Majumder

Electrical and Electronic Engineering, Bangladesh University of Engineering and Technology, Dhaka 1000, Bangladesh

Correspondence should be addressed to MD. Zoheb Hassan, dip.eee24@yahoo.com

Received 6 April 2011; Accepted 18 May 2011

Academic Editor: C. Carbonelli

This paper demonstrates an analytical approach on the bit error rate (BER) performance evaluation of a multi- carrier code division multiple access (MC-CDMA) communication link operating over terrestrial free space optical (FSO) channel considering effect of atmospheric turbulence The turbulence induced intensity fading is statistically modeled by Gamma-Gamma PDF (probability density function). Bit error rate performance improvement is proposed using photo detector spatial diversity with Equal Gain Combining (EGC) and Turbo Coding. Analysis is carried out with different bandwidth efficient phase shift keying (PSK) based sub-carrier intensity modulation (SIM) with direct detection. Numerical simulation results of proposed analytical model indicate that, sub-carrier intensity modulation scheme; number of receiver photo detectors, turbo coding parameter and link length should be optimally engineered for ensuring system reliability. It can be inferred from the simulation that, a reliable communication link (10^{-10} BER) can be established over a link length of 4 Km in strong turbulence fading condition using an array of 4 PIN photo detectors, 8-ary PSK based sub-carrier intensity modulation scheme and appropriate turbo coding parameter with an average 10.2 dB CINR (Carrier to Interference and Noise Ratio) requirement per photo detector. Besides, more than 130 dB average CINR gain is also confirmed from BPSK modulated, un-coded SISO (single input-single output) system for maintaining targeted BER (10^{-10}) in presence of strong turbulence fading.

1. Introduction

Free space optical communication (FSO) also known as wireless optical communication technique is a point to point to communication link in which two optical transceivers communicate via infrared laser light propagated through atmospheric channel. FSO recently has become a promising technology both for commercial as well as military application that can replete the gap between end user and backbone fiber optic infrastructure addressing the "last-mile" or "bottleneck" problem [1]. In metropolitan area network or local area network, end user is connected to the optical fiber network by means of existing DSL (digital subscriber line) having data speed in the range of Mbit/sec while FSO provides data rate in the rage of giga bit/sec. Besides addressing "bottle-neck" problem, FSO is also promising for transmitting RF signal over free space by means of subcarrier multiplexing (SCM). The present technology of transmission of radio signal over optical fiber link is multiplexing of several carriers in RF domain and transmitting over optical fiber link using intensity modulation, known as radio over fiber (RoF) technology. RoF technology is used for cable television and in satellite base stations. RoF technology can conveniently be replaced by radio over free pace optical (RoFSO) communication link using FSO system for transmitting RF signals excluding expensive use of optical fiber [2, 3]. The main advantage of FSO communication system is being free from license requirement, no fiber implementation cost, low power requirement, availability of cost-effective equipment, and almost the same performance of optical fiber network with a fraction of cost [4]. In simple words, FSO is a technology that combines high-speed performance

of optical communication and easy deployment of wireless communication system. For supporting multiple users with a reliable communication link, optical code division multiple access (OCDMA) has become a popular choice in optical fiber communication. CDMA has gained popularity from other multiple access system due to its ability to use the full available time, frequency and wavelength slot, and self-routing by the code sequence. Furthermore, application of multicarrier CDMA (MC-CDMA) also gained popularity in wireless communication by using transmission through several numbers of parallel frequency—nonselective fading channels avoiding channel delay spread. Transmission of CDMA signal through FSO link has gained attention in recent years' research because of the flexibility offered by FSO communication in terms of cost and performance. Performance of FSO-CDMA is reported in recent articles [5–7], and performance of Free space multicarrier OCDMA is reported in another recent article [8].

The main challenge of building FSO communication is the effect of atmosphere on the propagating light. The atmosphere contains aerosol and suspended water particle. The propagating light get absorbed, scattered, and deflected by these particles, and optical pulse attenuation takes place [9]. In dense atmosphere, this attenuation is as high as 270 db/km, where in clear atmosphere, it is only 0.043 db/km [10]. Pulse attenuation due to absorption is dependent on transmission wavelength, and the attenuation can be reduced by using the wavelength of lowest absorption window. The pulse attenuation due to scattering can simply be managed by increasing transmitting power [11]. The most severe challenge for FSO communication even in clear atmosphere is atmospheric turbulence-induced irradiance fluctuation. Atmospheric turbulence causes temperature gradient across the atmosphere, which causes change in refractive index of air. The change in refractive index causes phase and amplitude fluctuation of propagated light, which results beam scintillation, beam spread, and beam wander [12]. The irradiance fluctuation due to atmospheric turbulence is a statistical process, and a tractable model is necessary to describe it. Although simple power increase is sufficient for mitigating scattering and other link loss, it cannot improve link performance limited by turbulence-induced fading. In recent years, many techniques have been proposed such as maximum likelihood sequence detection (MLSD) [13] and diversity and error control coding with interleaving. Using spatial diversity at receiver BER performance of FSO communication link limited by γ-γ turbulence fading is evaluated in [14]. Hajjarian et al. [15] analysed bit error rate performance of multi-input multi-output (MIMO) FSO link over turbulence-induced fading channel. Channel coding for optical wireless link along with time diversity is also proposed to alleviate the effect of turbulence fading [16]. LDPC-(linear density parity check-) coded OFDM (orthogonal frequency division multiplexing) for FSO is proposed and was showed to outperform LDPC-coded OOK (on-off keying) FSO for weak to strong turbulence-fading condition [17].

Besides diversity and forward error correction coding, modulation scheme is also an important factor for reliability of FSO communication. In FSO, either intensity modulation or optical pulse modulation can be used. For simplicity of instruments, on-off keying- (OOK-) based intensity modulation is a widely used modulation scheme in FSO. But when the link is impaired by strong turbulence fading, random irradiance fluctuation requires adaptive threshold for OOK, which is difficult to acquire. Hence, subcarrier intensity modulation (SIM) is proposed, and it is reported that SIM exhibits better performance than OOK with less power requirement in the presence of atmospheric turbulence fading. Several recent articles have discussed implementation of SIM in atmospheric turbulence-fading condition. In [18], BPSK-modulated SIM using log-normal distributed intensity fading is discussed. BPSK-modulated SIM for γ-γ distributed fading channel is discussed in [19]. DPSK- (differential phase shift keying-) modulated SIM is also discussed for weak turbulence region in [20].

Now, previous contributions aimed to utilize diversity, error correction coding, and modulation scheme for the mitigation of turbulence induced fading and have already made this a well-investigated subject. But still, there is opportunity to carry out further research on this topic. Previous analysis have showed, with diversity in strong turbulence fading not less than 10^{-6}, that BER is achieved, and it requires almost equal or greater than 30–35 dB SNR [14, 18]. Definitely, this BER is not satisfactory for ensuring proper data communication and at the same time, this SNR requirement is very high. Another concern is bandwidth requirement, since application of coding needs extra bandwidth and the required system should be both bandwidth and power efficient for ensuring high rate and reliability. Increasing modulation order is an option to ensure bandwidth-bit rate efficiency, but this not power efficient, and obviously, there is some task of optimization to ensure both rate and reliability. Also, terrestrial link performance depends on link length between Tx and Rx, and it is expected that system should support more link length than conventionally achievable in worst situation with good reliability. These things are the motivation behind the current research.

In this paper an analytical approach is presented on BER performance evaluation of MC-CDMA communication link over turbulence fading limited FSO channel with receiver spatial diversity and turbo coding. The organization of this paper is following. Statistical model of atmospheric turbulence fading is presented in Section 2 and analytical model on bit error rate with Rx diversity is developed in Section 3. In Section 4 bit error rate performance of turbo coding with receiver diversity will be discussed. Numerical simulation results of proposed analytical model in previous sections will be discussed in Section 5 with a proposed profile of receiver, modulation scheme and turbo coding parameter. Finally, conclusion of present contribution will be discussed in Section 6.

2. Statistical Model of Atmospheric Turbulence-Induced Fading

Atmospheric circulation (due to distribution of temperature on the surface of earth) and wind flow (reason of atmospheric pressure and velocity variation) generate

atmospheric turbulence. Atmospheric turbulence produces eddies or small air pockets having randomly varrying refractive index. This refractive index variation causes phase perturbation of the wave front (isophase plane) of propagating light [15]. As a result, secondary waves generated from different point of wave front have different phase, and their interference with each other gives amplitude variation. In other words, air pockets will act as lenses for propagating light having different refractive indexes, and they will focus-defocus light randomly. The net result is that intensity of received optical signal will not be constant but fluctuating randomly similar to the amplitude fading due to multipath propagation in RF-wireless communication. Several statistical models are proposed to represent turbulence-induced intensity fading or irradiance fluctuation. For example, log-normal PDF, K distribution, and γ-γ PDF are the most used statistical model for presenting atmospheric turbulence-induced irradiance fluctuation. The weak turbulence is modelled by log-normal PDF, while strong turbulence is approximated by exponential model. Turbulence fading from weak to strong regime can be modelled very effectively by γ-γ distribution which represents received optical intensity $I = I_x I_y$, where I_x and I_y are, respectively, strong and weak eddies induced intensity fading statistically modelled by γ distribution. γ-γ PDF for turbulence-induced irradiance fluctuation is as follows [21]

$$f(I) = \frac{2(\alpha\beta)^{(\alpha+\beta)/2}}{\Gamma(\alpha)\Gamma(\beta)} I^{((\alpha+\beta)/2)-1} K_{(\alpha-\beta)}\left(2\sqrt{(\alpha\beta)I}\right), \quad (1)$$

where I is the signal intensity, $\Gamma()$ is the γ function, and $K_{\alpha-\beta}$ is the modified Bessel function of the second kind of order $\alpha - \beta$. Here, α and β are the effective number of small- and large-scale eddies of the scattering environment. These parameters can be directly related to atmospheric conditions according to [21]

$$\alpha = \left[\exp\left(\frac{0.49\sigma_x^2}{\left(1 + 1.11\sigma_x^{12/5}\right)^{(7/6)}}\right) - 1\right]^{-1}, \quad (2)$$

$$\beta = \left[\exp\left(\frac{0.51\sigma_x^2}{\left(1 + 0.69\sigma_x^{12/5}\right)^{5/6}}\right) - 1\right]^{-1}. \quad (3)$$

Irradiance fluctuation due to atmospheric turbulence is known as scintillation, and σ_x^2 is called scintillation index. Therefore, this parameter directly indicates strength of atmospheric turbulence. This parameter is defined as normalized variance of intensity fluctuation; that is, $\sigma_x^2 = E[I^2]/E[I]^2 - 1$. In many literatures, this scintillation index is directly related to channel parameter and system parameter by this equation $\sigma_x^2 = 1.23C_n^2k^{7/6}L^{11/6}$ [19]. In this equation, C_n^2 is atmospheric refractive index structure parameter, k ($= 2\pi/\lambda$, λ is wavelength) is wave number, and L is link length. Value of atmospheric refractive structure parameter depends on channel condition and for terrestrial link, it varies from $10^{-13}m^{-2/3}$ to $10^{-17}m^{-2/3}$ referring strong-to-weak turbulence-induced irradiance fluctuation. For constant atmospheric refractive structure parameter, scintillation index is completely dependent on link length L, since wavelength of light is constant. Now, the value of α and β is completely dependent on scintillation index, and the value of these parameters directly indicates the nature of atmospheric turbulence. Consequently, impact of atmospheric turbulence can be very effectively described with these parameters.

3. Analytical Model on Bit Error Rate with Rx Diversity

This section is organized into three parts. In the first part, transmitter model considered for present analysis will be discussed. In next part, CINR performance with receiver diversity and equal-gain combining will be discussed, and finally, bit error rate evaluation with BPSK and higher-order PSK-based subcarrier intensity modulation will be discussed.

3.1. Transmitter Model. Schematic block diagrams of transmitter and receiver with diversity and turbo encoding are illustrated in Figures 1(a) and 1(b), respectively. In transmitter bit stream from a particular user is first encoded by turbo coding and mapped into a PSK (phase shift keying) signaling constellation. If BPSK (binary phase shift keying) is used then output will take only $+1$ or -1 values. On the other hand, for higher order PSK mapping it will take complex value from corresponding constellation diagram. This turbo encoded and PSK mapped sequence then goes into serial to parallel conversion. Each parallel component is multiplied by a chip of user dependent spreading sequence and modulated by orthogonal sub-carries having centre frequency f_c and separated by $2\pi F/T_b$ from each other. F can take any integer value. If $F = 1$ the system will be identical with OFDM (Orthogonal frequency division multiplexing). For present analysis F is considered to take integer values greater than or equal to 2 which allows transmitter operating in continuous region in stead of using FFT block similar to OFDM. This process is carried out for all available user data and outputs of all users are summed together which plays the role of sub-carrier multiplexed RF signal that drives the laser diode after adding with DC bias. If P_t is average transmitted optical power (un-modulated optical carrier power) and ε is optical modulation index (OMI) then transmitted optical power waveform will be [5]

$$x(t) = P_t(1 + \varepsilon m(t)), \quad (4)$$

where $m(t)$ is message signal shown in

$$m(t) = \sum_{k=1}^{K} \sqrt{\frac{2P_c}{M}} \sum_{m=0}^{M-1} b_k[m]c_k[m] \cos\left(2\pi f_c t + 2\pi \frac{F}{T_b} t\right). \quad (5)$$

In the above equation, K is the number of total available users, M is the number of orthogonal subcarriers (it is also number of chips of spreading sequence), and P_c is RF-carrier

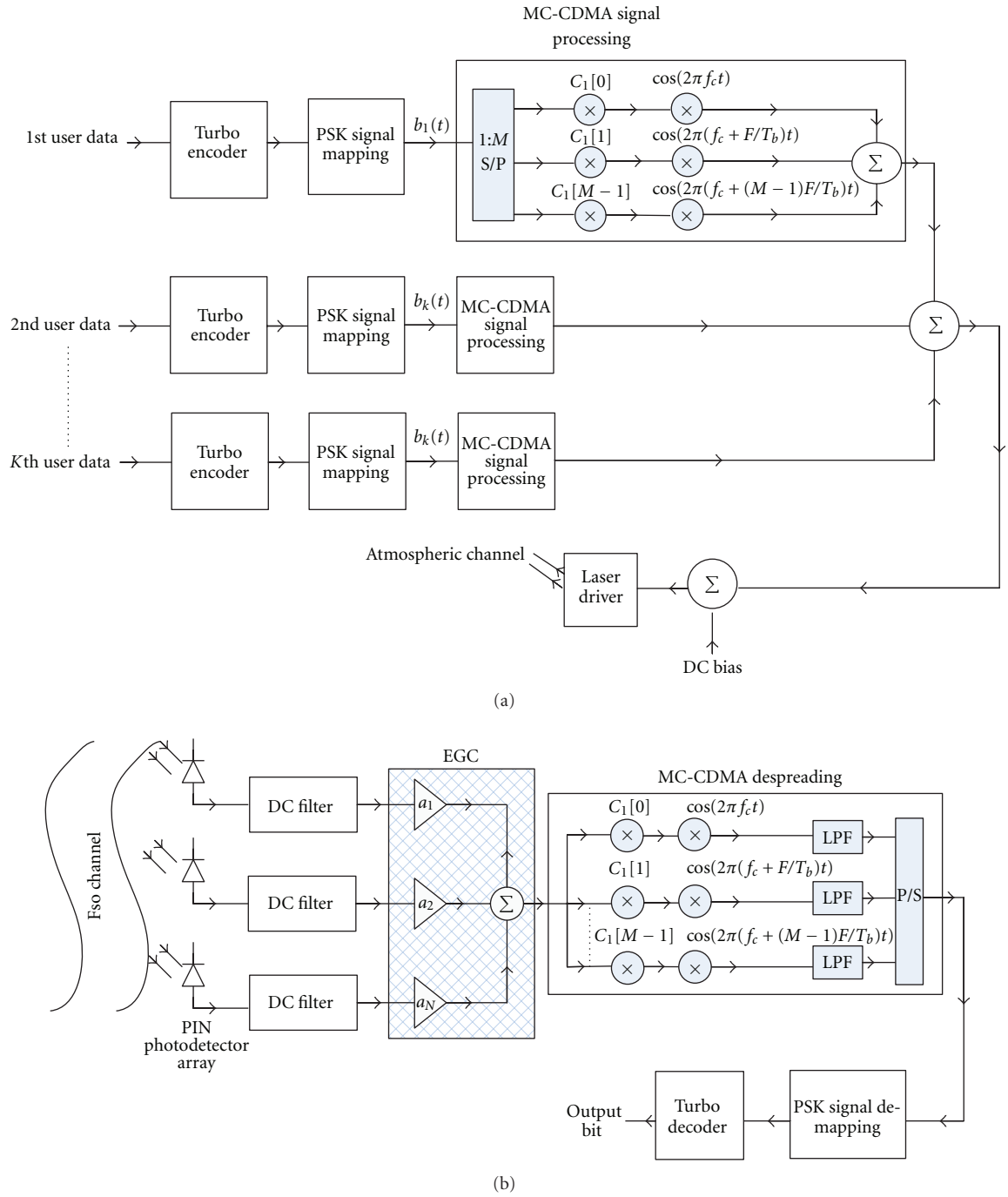

Figure 1: (a) Schematic Block diagram of Transmitter for transmission of turbo-coded MC-CDMA signal over FSO link using intensity modulation and (b) Receiver with photo detector space diversity and turbo decoding.

power. Data sequence and code sequence for kth user are, respectively, indicated by b_k and c_k. In order to avoid laser diode going into saturation region, it is required to chose optical modulation index and RF-carrier power in such a way that ensure $|\varepsilon m(t)| \leq 1$ [17]. In [5], authors showed that the value of optical modulation index determines received carrier to interference and noise ratio (CINR). According to them, there is an optimum value of OMI for a particular received power for which CINR attains maximum value.

3.2. CINR Performance with Receiver Diversity and Equal Gain Combining. The channel considered for transmission of light wave in free space is atmospheric turbulence limited intensity fading channel. Irradiance fluctuation or scintillation due to atmospheric turbulence is statistically modelled by γ-γ PDF which is described in Section 2. Besides random intensity fluctuation, this channel also causes beam wander and beam spread. These effects result "beam spot" on the receiver plane not confined to a single point

(which is the result in the absence of turbulence fading) but gets randomly divided into multiple zone of high and low intensity. Alternatively, instead of being concentrated to the focal point, received optical power gets distributed over the focal plane of the receiver, and consequently, receiver collects only a small portion of transmitted optical power. One potential solution of this problem is increasing receiver diameter by means of averaging over the turbulence distorted optical field. This is known as "aperture averaging". For weak-to-medium turbulence-fading strength region, aperture averaging is effective to combat against the deleterious effect of turbulence fading. But because of huge distortion of received optical field in the presence of strong turbulence fading, it is not possible to depend only on aperture averaging. In this situation, spatial diversity becomes an excellent and easily deployable solution. Spatial diversity requires multiple photodetectors of small size in receiver instead of a single receiver so that each one can collect a portion of transmitted optical power, and after proper diversity combining, they can minimize fading-induced error. The success of spatial diversity system in fading channel depends on the correlation among the receivers. In order to ensure uncorrelated turbulence fading experienced by each receiver, it is required to place each photodetector from its neighbour at least one beam correlation length. In strong turbulence-fading condition, this distance is not more than some few centimetres, since this parameter is proportional to Fried's parameter r_0 defined as $r_0 = 1.68(C_n^2 Lk^2)^{-3/5}$ and, consequently, inversely proportional to turbulence strength [22]. As a result, ensuring minimum spatial separation among the photodetectors for having uncorrelated fading is practically achievable [15, 23]. Besides, the dimension of each receiver should be chosen so that total noise generated after diversity combining does not exceed noise generated with a single large receiver system.

Now, receiver is assumed to have an array of N number of P.I.N photo detectors placed at a distance of one beam correlation length from each other, and therefore, the correlation among photodetectors can be neglected. Block diagram of such diversity system is illustrated in Figure 1(b). If R is the responsivity of photodetector, then photocurrent generated from nth photodetector is as follows:

$$i_n(t) = RP_r I_n\left(1 + \varepsilon m(t)e^{j\theta_n}\right) + n_n(t). \tag{6}$$

In (6), P_r is received optical power (difference between P_r and P_t indicates link loss of optical power), I_n is irradiance fluctuation experienced by nth photodetector statistically modelled as γ-γ PDF (1), $n_n(t)$ is the noise current generated from photodetector (mainly consists of thermal noise and background radiation shot noise), and θ_n is for phase shift due to propagation delay. Now, after DC filter out and downconversion, electrical signal generated from each photodetector are combined with equal gain combining (EGC). Tap coefficient of each branch of equal gain combiner is set having unity gain and conjugate phase of corresponding signal; that is, $a_i = e^{-j\theta_i}$, where $i = 1, 2, \ldots N$. Fading channel coefficients estimation for EGC is a challenging task, and it influences system performance. Discussion of fading channel coefficients estimation for EGC is out of the scope of present paper, and ideal estimation is assumed here for simplicity. Output signal $i(t)$ generated from EGC block is as follows:

$$\begin{aligned} i(t) &= \sum_{n=1}^{N} i_n(t)e^{-j\theta_n} \\ &= RP_r\varepsilon m(t)\sum_{n=1}^{N} I_n + \sum_{n=1}^{N} n_n(t)e^{-j\theta_n} \\ &= RP_r\varepsilon m(t)I_t + n(t). \end{aligned} \tag{7}$$

Here, $n(t)$ is the total noise current after equal gain combining. $I_t = \sum_{n=1}^{N} I_n$ is the total received intensity collected by all photodetectors after linear combining. In this case, it is assumed each photodetector to experience independent intensity fading, because their spatial separation ensures that. Therefore, I_t can be considered as the sum of N number of i.i.d (independent and identically distributed) random variables following γ-γ distribution. Calculation of PDF (probability density function) of I_t is important, since it will be used to determine PDF of CINR which will be used to evaluate bit error rate (BER) performance. Now, for the sum of large number of i.i.d random variables, according to central limit theorem PDF will be Gaussian. In [24], Chatzidiamantis et al. have proposed a better approach for determining PDF of a sum of γ-γ distributed variables. According to them, for i.i.d. case, sum of γ-γ distributed variables will follow another γ-γ distribution with parameters (α_t, β_t, w_t), where constitute variables follow γ-γ distribution (2) with parameters(α, β, w). Here, w is the mean of γ-γ distribution, and for (2), $w = 1$. The relation among these parameters is listed below:

$$\begin{aligned} \alpha_t &= N\alpha + (N-1)\left(\frac{-.127 - .95\alpha - .0058\beta}{1 + .00124\alpha + .98\beta}\right), \\ \beta_t &= N\beta, \\ w_t &= Nw = N. \end{aligned} \tag{8}$$

PDF of I_t will be as follows:

$$\begin{aligned} f(I_t) = {} & \frac{2(\alpha_t\beta_t)^{(\alpha_t+\beta_t)/2}}{\Gamma(\alpha_t)\Gamma(\beta_t)N^{(\alpha_t+\beta_t)/2}}(I_t)^{((\alpha_t+\beta_t)/2)-1} \\ & \times K_{(\alpha_t-\beta_t)}\left(2\sqrt{\frac{(\alpha_t\beta_t)}{N}I_t}\right). \end{aligned} \tag{9}$$

Output signal form EGC block can be written using (5) into (7)

$$\begin{aligned} i(t) = {} & RP_r I_t\varepsilon\sum_{k=1}^{K}\sqrt{\frac{2P}{M}}\sum_{m=0}^{M-1} b_k[m]c_k[m] \\ & \times \cos\left(2\pi f_c t + 2\pi\frac{F}{T_b}t\right) + n(t). \end{aligned} \tag{10}$$

After equal gain combining, signal is passed to MC-CDMA despreading block (Figure 1(b)), where opposite

function of MC-CDMA spreading is done. It is assumed receiver is tuned for uth user. Decision variable for uth user will be as follows:

$$\begin{aligned} z_u(t) &= \frac{1}{T_b}\int_0^{T_b}\sum_{m=0}^{M-1} i(t)c_u[m]\cos\left(2\pi f_c t + 2\pi\frac{F}{T_b}t\right)dt \\ &= RP_rI_t\varepsilon\sqrt{\frac{P}{2M}}\sum_{m=0}^{M-1} b_u[m]c_u^2[m] \\ &\quad + RP_rI_t\varepsilon\sum_{k=1,k\neq u}^{K}\sqrt{\frac{P}{2M}}\sum_{m=0}^{M-1} b_k[m]c_k[m]c_u[m] \\ &\quad + \frac{1}{T_b}\int_0^{T_b}\sum_{m=0}^{M-1} n(t)c_u[m]\cos\left(2\pi f_c t + 2\pi\frac{F}{T_b}t\right)dt \\ &= S + \mathrm{MAI} + n_1. \end{aligned} \tag{11}$$

Here, first term is for signal term, 2nd term represents multiaccess interference (MAI), and third term will be noise current. Since it is assumed that a large number of users present, so from central limit theory, multiaccess interference will be Gaussian with zero mean and variance σ^2_{MAI}. Noise will also be Gaussian with zero mean and variance $\sigma^2_{n_1}$

Using the above approximation from (11), the following terms are found:

Signal power,

$$S^2 = (RP_r\varepsilon)^2\frac{P}{2M}\left(\sum_{m=0}^{M-1} c_u^2[m]\right)^2 I_t^2 = \frac{1}{2}(RP_r\varepsilon)^2PMI_t^2, \tag{12}$$

multiaccess interference variance,

$$\begin{aligned} \sigma^2_{\mathrm{MAI}} &= (RP_r\varepsilon)^2\frac{P}{2M}\sum_{k=1,k\neq u}^{K}\sum_{m=0}^{M-1}\left(E[c_k[m]c_u[m]]\right)^2E[I_t^2] \\ &= \frac{1}{2}(RP_r\varepsilon)^2(K-1)P\beta_{k,u}^2E[I_t^2]. \end{aligned} \tag{13}$$

In the above equation, $E[I_t^2]$ is the second-order moment of I_t, representing mean-square value of channel statistics. It is defined as $E[I_t^2] = 1/\alpha_t + 1/\beta_t + 1/\alpha_t\beta_t$. Normalized cross-correlation between spreading sequence of uth user and kth user is defined as $\beta_{k,u}$. This parameter takes value from 0 to 1 representing best case (no MAI) to worst case (maximum multiaccess interference).

Noise from photo detector consists of mainly thermal noise and shot noise due to both received power and background radiation. Therefore noise variance will be

$$\sigma^2_{n_1} = \sigma^2_{\mathrm{thermal}} + \sigma^2_{\mathrm{shot}}. \tag{14}$$

Thermal noise variance is defined as follows:

$$\sigma^2_{\mathrm{thermal}} = \frac{4KT}{R_L}B. \tag{15}$$

Shot noise variance is defined as follows:

$$\sigma^2_{\mathrm{shot}} = 2eR(\varepsilon P_r + I_B)B. \tag{16}$$

Different notations used for noise variance are explained below:

R = photodetector responsivity, B = bandwidth of the signal, K = Boltzmann constant, e = charge of electron, I_B = background noise current, T = temperature, R_L = load resistance of photodetector.

CINR (γ) of the system is given below:

$$\begin{aligned} \gamma &= \frac{S^2}{\sigma^2_{\mathrm{MAI}} + \sigma^2_{n_1}} \\ &= \frac{(1/2)(RP_r\varepsilon)^2PMI_t^2}{(1/2)(RP_r\varepsilon)^2(K-1)P\beta_{k,u}^2E[I_t^2] + \sigma^2_{n_1}} \\ &= CI_t^2. \end{aligned} \tag{17}$$

Here, C is constant term providing CINR without effect of turbulence fading. It is referred as average electrical CINR per photodetector and has the following expression:

$$C = \frac{(1/2)(RP_r\varepsilon)^2PM}{(1/2)(RP_r\varepsilon)^2(K-1)P\beta_{k,u}^2E[I_t^2] + \sigma^2_{n_1}}. \tag{18}$$

From expression of C, it is seen by increasing M (number of orthogonal subcarrier) that it is possible to reduce interference. Actually, this benefit is earned due to increase of processing gain of system.

Next PDF of CINR need to be determined, since it will be used for average BER evaluation. From expression of CINR(γ) , it is seen, the only random variable present is I_t. Hence, using simple variable transformation it is possible to show that SINR obeys the following PDF:

$$\begin{aligned} f_\gamma(\gamma) &= \frac{f_{I_t}\left(\sqrt{\gamma/C}\right)}{2\sqrt{\gamma C}} \\ &= \frac{1}{2\sqrt{\gamma C}}\frac{2(\alpha_t\beta_t)^{(\alpha_t+\beta_t)/2}}{\Gamma(\alpha_t)\Gamma(\beta_t)N^{(\alpha_t+\beta_t)/2}}\left(\sqrt{\frac{\gamma}{C}}\right)^{((\alpha_t+\beta_t)/2)-1} \\ &\quad \times K_{(\alpha_t-\beta_t)}\left(2\sqrt{\frac{(\alpha_t\beta_t)}{N}\sqrt{\frac{\gamma}{C}}}\right). \end{aligned} \tag{19}$$

3.3. Bit Error Rate Evaluation. For BPSK-based signal mapping conditional, bit error rate expression is as follows [25]

$$P_{e/\gamma}\left(\frac{e}{\gamma}\right) = \frac{1}{2}\,\mathrm{erfc}\left(\sqrt{\frac{\gamma}{2}}\right). \tag{20}$$

BPSK signalling is not bandwidth efficient, since it requires a bandwidth (one sided) equal to transmission bit rate and has unity spectral efficiency (bit/s/Hz). Spectral efficiency of a modulation scheme is defined as the ratio of transmission bit rate to required bandwidth. Due to

the scarcity of bandwidth specially, when error correction coding is applied, spectral efficiency of the system need to be increased. In order to achieve higher spectral efficiency than unity, multilevel modulation scheme has been proposed. M-ary PSK is a candidate for such modulation scheme borrowing the idea of phase shift keying in multilevels rather than two levels. In M-ary PSK signalling, $\log_2 M$ bits are selected from input bit stream, and they are mapped to a complex point of a circular constellation diagram consisting M-points. As a result, generated symbol has a period T which has the following relation with bit period T_b:

$$T = T_b \log_2 M. \tag{21}$$

Bandwidth required by this system is as follows:

$$B = \frac{1}{T} = \frac{1}{T_b \log_2 M} = \frac{R_b}{\log_2 M}. \tag{22}$$

System spectral efficiency

$$\eta = \frac{R_b}{B} = \log_2 M. \tag{23}$$

This spectral efficiency considers one-sided bandwidth, while it will be half of present if two sided bandwidth is considered. Spectral efficiency of M-ary PSK system can be increased by increasing values of M, where M takes 4, 8, 16, 32, 64, and so on. For QPSK system ($M = 4$), (23) reveals spectral efficiency of order 2. That means that QPSK system requires half bandwidth than corresponding BPSK system, or it can support double transmission bit rate if same bandwidth is used. This bandwidth saving property is very advantageous when coding is used for a bandwidth limited channel.

Like two level modulation scheme, it is difficult to find a closed form expression of bit error rate for M-ary PSK system. For medium-to-high SINR region, BER for M-ary PSK system is approximated to the following error function using union bound approach [25]:

$$P_{e/\gamma}\left(\frac{e}{\gamma}\right) = \frac{1}{k}\operatorname{erfc}\left(\sqrt{\frac{k\gamma}{2}}\sin\left(\frac{\pi}{M}\right)\right). \tag{24}$$

Here, $k = \log_2 M$

For either BPSK or M-ary PSK unconditional, average bit error rate can be found by integrating conditional bit error rate (20), and (24) over the PDF model of CINR proposed by (19). So, average BER can be computed from

$$P_e = \int_0^\infty P_{e/\gamma}\left(\frac{e}{\gamma}\right) f_\gamma(\gamma)\, d\gamma. \tag{25}$$

Since it is not possible to obtain a simple closed from expressions from the above equation, average BER will be computed by numerical integration of (25) and will be discussed in Section 5.

4. Performance of Turbo Coding with Rx Diversity

The role of error correction coding (known as channel coding) is to increase system robustness against noise and interference. Besides multiple photo detectors, error correction coding has been also proposed to improve link performance limited by strong turbulence fading [26, 27]. Several types of error-correction coding have been proposed in recent years for optical wireless link. For example, Convolutional code, Reed-Solomon (RS) code, Turbo & LDPC (Linear Density Parity Check) Code. It is found in presence of weak turbulence typical Convolutional or RS code performs well, but strong turbulence fading requires more complex code like LDPC or turbo code. It is well known that channel coding is not sufficient to completely mitigate fading. Diversity is required to mitigate fading and integration of fading and channel coding has become a mature technology for overcoming fading induced error. For channel coding, turbo coding is chosen in current analysis since its near Shannon performance and availability of encoder decoder in UMTS/3G communication system. Details of turbo encoding-decoding process will be found in [28, 29]. For present content, discussion of bit error rate performance of turbo coding is more relevant than architecture.

Bit error performance of turbo or turbo like concatenated codes is discussed in several articles [30–32]. Bit error rate performance of turbo code delineates two regions. The first region is "low SNR" region, in which BER gets decreased sharply due to slight increase of SNR. This "waterfall decrease" of BER is followed by a region limited by medium to high SNR value. In this region, BER performance curve coincides with "error floor" (also known as asymptotic BER) described by a Gaussian $-Q$ function. Since this SNR region is mostly typical in practical situation, it is chosen for current analysis. Another reason behind the choice, this error floor is an alternative to a large time consuming simulation for obtaining very low BER (10^{-10}) in this SNR region [32].

"Error-floor" or Asymptotic BER of turbo code in medium to high CINR region for BPSK modulation can be expressed by following equation using ML(maximum likelihood) decoding (which is very close to iterative decoding) [30, 32]:

$$P\left(\frac{e}{\gamma}\right) \le \frac{1}{2}\sum_{d=d_{\text{free}}}^{2(v+N_{\text{int}})} \frac{N_d w_d}{N_{\text{int}}}\operatorname{erfc}\left(\sqrt{\frac{dr\gamma}{2}}\right). \tag{26}$$

Here, d is code weight, and N_d is the number of codewords with weight d and N_{int} is interleaver block size. For PCCC turbo code, error-floor performance bound is dominated by code-effective free distance d_{free} than the other terms for which $d \neq d_{\text{free}}$. So the above bound is simplified in (27) for error-floor performance of turbo code in medium to high CINR region for BPSK modulation

$$P\left(\frac{e}{\gamma}\right) = \frac{1}{2}\frac{w_{\text{free}}}{N_{\text{int}}}\operatorname{erfc}\left(\sqrt{\frac{d_{\text{free}} r\gamma}{2}}\right). \tag{27}$$

For M-ary PSK modulation the above expression is modified as follows:

$$P\left(\frac{e}{\gamma}\right) = \frac{1}{k}\frac{w_{\text{free}}}{N_{\text{int}}}\operatorname{erfc}\left(\sqrt{\frac{k d_{\text{free}} r\gamma}{2}}\sin\left(\frac{\pi}{M}\right)\right). \tag{28}$$

Table 1: Parameters of rate-1/3 16 state turbo code with interleaver size N [32].

N	x	$\overline{d_{\text{free}}}$	$d_{\text{free}}^{\text{best}}$	$w_{\text{free}}^{\text{best}}$
2	2	8.000	8	2
3	6	8.000	8	2
4	24	8.917	11	7
5	120	8.933	10	3
6	720	9.269	11	7
7	5040	9.331	12	23
8	40320	9.403	12	12
9	362880	9.551	12	4
10	3628800	9.708	13	29
20	10000	10.974	14	21
40	10000	12.300	16	8
80	10000	13.354	18	4
160	10000	14.547	21	6
320	10000	16.190	23	1
640	10000	18.032	28	7
1280	500	19.711	30	14

In (27) and (28), d_{free} is the code-free distance defined as the minimum hamming distance between code words which coincides with minimum hamming weight of a nonzero code word for linear code. N_{free} is the code multiplicity defined as the number of code words having weight as d_{free}. w_{free} is defined as information bit multiplicity defined as sum of hamming weights of N_{free} information frames generating code words with weight d_{free}. Code rate is noted by r, defined as $r = k/n$, where k and n are, respectively, number of input bits and output coded bits.

In order to evaluate asymptotic BER analytically, it is required to calculate above parameters. This is done by Garello et al. [32]. The author's finding for 16 state rate-1/3 turbo code having two constitute rate-1/2 RSC (recursive systematic convolutional) code is illustrated in Table 1. RSC code has following transfer function $(1, n(D)/g(D))$ where $n(D) = 1 + D + D^2 + D^3 + D^4$ and $g(D) = 1 + D^3 + D^4$. (In octal, they are, respectively, 37 and 23).

In Table 1, x is total number of available interleavers of N_{int} size, $\overline{d_{\text{free}}}$ is the average code free distance over all possible free distances for fixed size of interleaver; that is, $\overline{d_{\text{free}}} = \sum_{i=1}^{N_{\text{int}}} d_{\text{free}}(i)/x$, $d_{\text{free}}^{\text{best}}$ is the best (maximum) free distance among them and $w_{\text{free}}^{\text{best}}$ is the minimum value from all possible values of information bit multiplicity for a fixed interleaver size.

Error floor performance of turbo code has two issues: first one is size or length of interleaver, and second one is free distance and other parameters (which actually depends on design the interleaver) for a fixed length of interleaver. These issues will be discussed in numerical simulation part. From Table 1, for each interleaver, there is a pair of maximum free distance and minimum information bit multiplicity for which error floor performance of turbo code will be optimum for that particular length of interleaver. Consequently, d_{free} and w_{free} of (27) and (28) will be replaced by $d_{\text{free}}^{\text{best}}$ and $w_{\text{free}}^{\text{best}}$, respectively, for performance evaluation.

Table 2: Parameters related to nature of atmospheric turbulence-induced fading [19].

Parameter	Strong turbulence	Medium turbulence	Weak turbulence
σ_x^2	3.5	1.6	0.2
α	4.22	4.02	11.2
β	1.4	1.9	10

Table 3: Simulation parameters related to system configuration.

Parameter	Value
Spreading sequence	GOLD
Number of chips (number of orthogonal subcarrier)	256
Number of user	250
Photodetector responsivity	0.85 A/W
Optical modulation index	0.6
Background limited shot noise	10^{-15} watt
Temperature	300 K
Load resistance (RL)	50 ohm
Bandwidth	1.25 G bps

Now, average bit error rate for present system with receiver diversity and turbo coding can be found by integrating (27) and (28) over PDF of CINR proposed in (19). Consequently, the following two equations are found for unconditional bit error rate, and they will be evaluated by means of numerical integration:

$$P_{e\text{-BPSK}} = \int_0^\infty \frac{1}{2}\frac{w_{\text{free}}^{\text{best}}}{N_{\text{int}}}\,\text{erfc}\left(\sqrt{\frac{d_{\text{free}}^{\text{best}} r\gamma}{2}}\right) f_\gamma(\gamma)\,d\gamma,$$

$$P_{e\text{-MPSK}} = \int_0^\infty \frac{1}{k}\frac{w_{\text{free}}^{\text{best}}}{N_{\text{int}}}\,\text{erfc}\left(\sqrt{\frac{k d_{\text{free}}^{\text{best}} r\gamma}{2}}\sin\left(\frac{\pi}{M}\right)\right) f_\gamma(\gamma)\,d\gamma. \tag{29}$$

5. Numerical Results and Discussion

Following theoretical analysis on Sections 3 and 4, average bit error rate and other system performance parameters are numerically evaluated in this section. Parameters related to strength of atmospheric turbulence used throughout the numerical evaluation are listed in Table 2. Simulation parameters related to system configuration are listed in Table 3.

Figures 2, 3, 4 and 5 are found by numerical integration of (25) for different system parameters. In Figure 2, BER performance against average electrical CINR is illustrated for BPSK intensity modulated FSO system without diversity and coding. It is seen, in weak turbulence 10^{-8} BER is achieved with 30 dB CINR requirement. On the other hand, for strong turbulence fading with 30 dB average CINR only 10^{-2} BER is achieved which is obviously unacceptable for reliable communication. Hence, diversity and coding must be employed to improve link performance limited by strong turbulence fading.

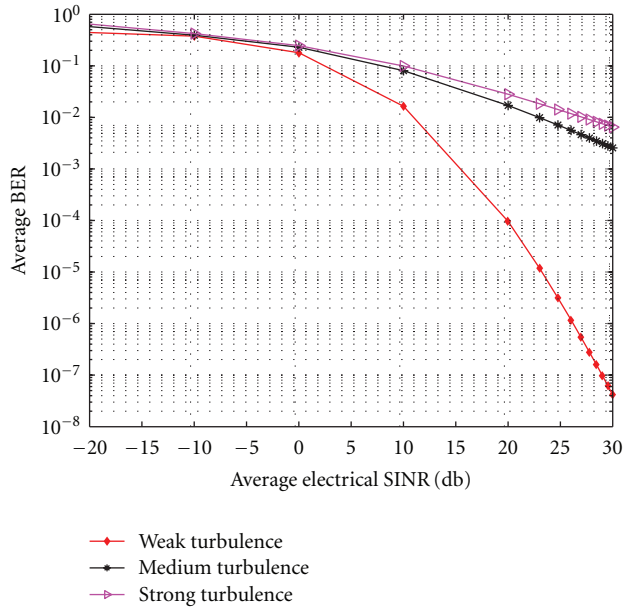

Figure 2: Average BER for SISO, un-coded, BPSK-modulated FSO system in different turbulence strength conditions.

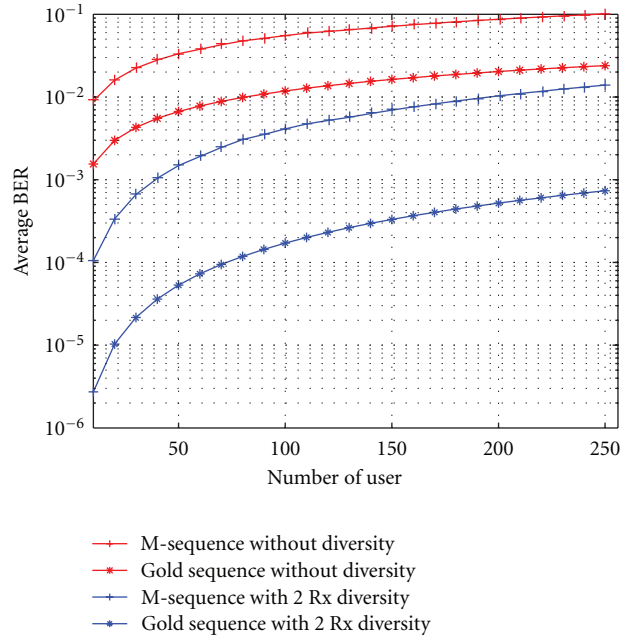

Figure 3: Average BER against number of users for −20 dBm received optical power with BPSK modulated and un-coded system in presence of strong turbulence fading.

Figure 3 is an illustration of average BER against number of users with −20 dBm received optical power considering strong turbulence fading. Here BPSK intensity modulated, un-coded system is employed with 256 chip gold and m-sequence. System using gold sequence outperforms system with m-sequence since former one exhibits lower cross-correlation and hence lower MAI. For gold sequence with single Rx, BER becomes more than 10^{-2} when number of user approaches up to 100. This unacceptable condition is improved when 2 Rx with EGC are used with same system configuration.

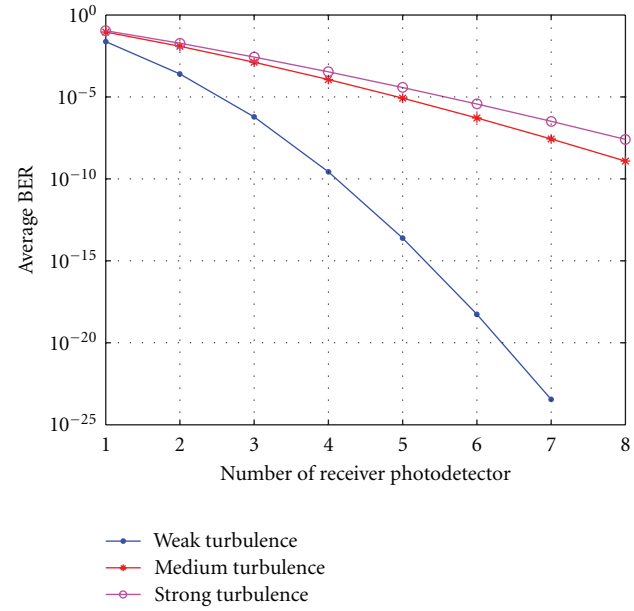

Figure 4: BER performance for variation of number of photo detectors with fixed average CINR (10 dB) in different turbulence strength conditions.

Using spatial diversity of photo detectors in Figure 4, BER performance is profiled against number photo detectors for a fixed CINR (10 dB) in different turbulence conditions. For weak turbulence regime, it is possible to achieve 10^{-10} BER with an array of 4 photo detectors and for strong turbulence regime, a complex structure of 8 receiving photo detectors gives a more appealing BER (10^{-8}) than SISO. Obviously, diversity is a very effective solution for improving system reliability without increase of received CINR requirement.

Above figures (Figures 2 to 4) deal with BPSK based intensity modulation. In order to achieve higher spectral efficiency (bit/s/Hz) or bandwidth efficiency, modulation order should be increased. In Figure 5 BER performance evaluation is illustrated with different PSK based intensity modulation for un-coded FSO system when strong turbulence fading is suffered by system. Higher order modulation scheme shows appealing performance in terms of bit rate-bandwidth efficiency (23). But this performance is earned by increasing transmitted power to provide same reliability with lower order modulation scheme (24). This is illustrated in Figure 5(a) where performance of 4, 8 and 16-PSK based intensity modulated FSO system with 2 photo detectors are displayed and it is seen lower order PSK outperforms higher order PSK system in terms of power requirement for same BER. Hence higher order modulation schemes are bandwidth efficient but not power efficient. Power efficiency of these systems can be increased by increasing diversity order. In Figure 5(b), 8-ary PSK based SIM with 4 photo detectors outperforms QPSK with 2 Rx and 16-ary PSK with 5 photo detectors outperforms both QPSK and 8-ary PSK in terms of

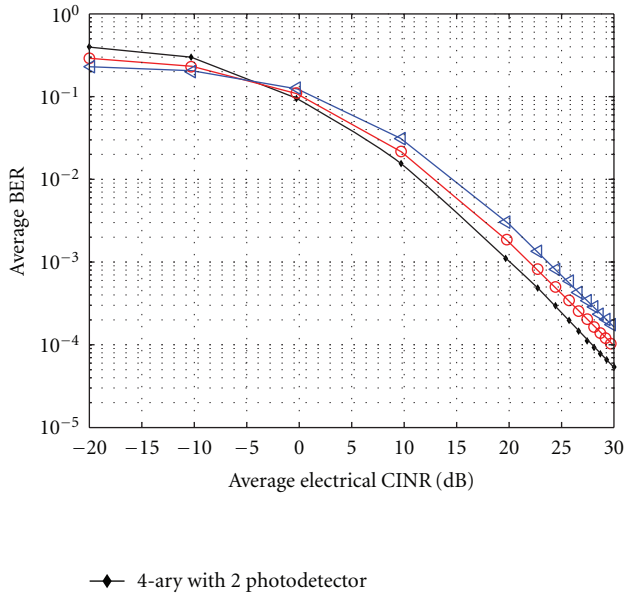

(a)

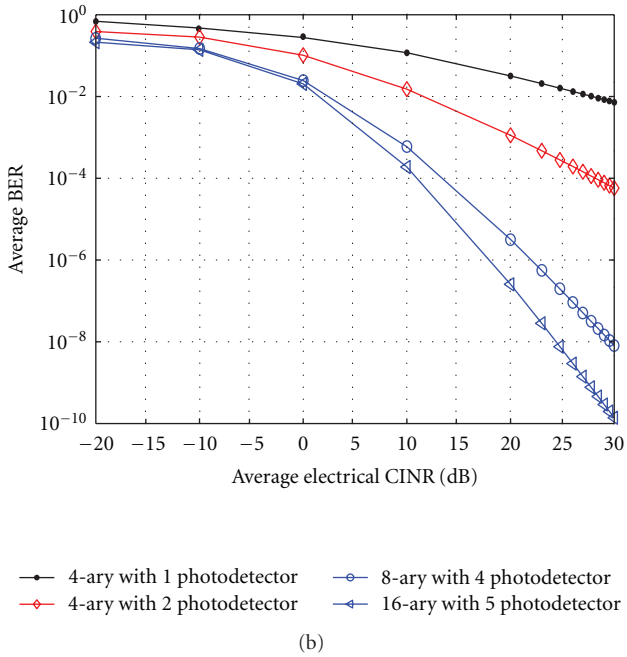

(b)

Figure 5: BER performance for different PSK- based sub-carrier intensity modulated and un-coded FSO system in presence of strong turbulence fading (a) with same photo detector number and (b) with different photo detector number.

bit error rate. 8-ary PSK system offers three times bandwidth efficiency and 16-ary PSK offers four time bandwidth efficiency than BPSK system. Consequently, improvement of BER performance and spectral efficiency of system are simultaneously offered by employment of diversity.

Figures 6–9 are found by numerical integration of (29) and (18) for different system parameters. In Figure 6 BER performance comparison between with and without turbo

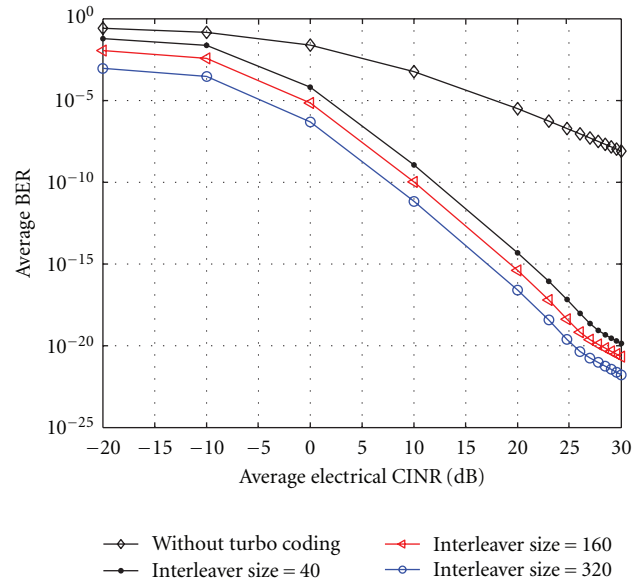

Figure 6: BER performance comparison for 8-ary PSK based intensity modulated FSO system using 4 photo detectors with and without turbo coding in presence of strong turbulence fading.

coding is profiled in presence of strong turbulence fading condition. Here rate-1/3 turbo code is used which requires three times extra bandwidth then conventional system. This bandwidth requirement is compensated by employing 8-ary PSK based sub-carrier intensity modulation scheme with an array of 4 photo detectors at receiver. In Figure 6 three candidates of turbo coding having following parameters are used: $(N_{\text{int}}, d_{\text{free}}^{\text{best}}, w_{\text{free}}^{\text{best}} = (40, 16, 4), (160, 21, 6), (320, 23, 1)$. It is seen turbo code with interleaver size $N = 320$ shows more appealing performance than other candidates. In strong turbulence fading condition turbo coding with this parameter offers a very good BER (10^{-10}) with approximately only 7.5 dB average CINR requirement. Consequently, this coding parameter is chosen for further system performance evaluation. In practice, free distance and information bit multiplicity parameter discussed above depends on the design of a interleaver of a particular length. The design issue of a interleaver for obtaining best performance from turbo code is out of the scope of present analysis. Only the design goal of interleaver for obtaining best performance from turbo code is discussed here in terms of above parameters.

Now it is found FSO system using 8-ary PSK based sub-carrier intensity modulation with 4 photo detectors at receiver and turbo coding with interleaver size $N = 320$ shows a very appealing performance in strong turbulence fading condition. Table 4 also illustrates a profile showing CINR gain for obtaining 10^{-10} BER from BPSK modulated, SISO and un-coded system in various turbulence condition (with variation of scintillation index). From this table, it is seen for targeted BER (10^{-10}) with proposed system configuration average CINR requirement varies from 1 dB to 7.7 dB when turbulence strength varies from weak to strong. At the same time CINR gain is confirmed to be 137.8 dB to 56.9 dB from strong to weak turbulence regime.

Table 4: CINR gain in various turbulence strength regimes for targeted BER (10^{-10}).

Scintillation index σ_x^2	Average CINR (dB) Requirement for BPSK-modulated, SISO, and un-coded system	Average CINR (dB) requirement for 8-ary PSK-modulated, SIMO(4 order diversity), and Turbo-coded ($N = 320$) system	CINR gain (dB)
3.5	145.5	7.7	137.8
3	138.8	7.3	131.2
2.5	130.5	6.7	123.8
2.0	119.5	6.0	113.5
1.5	104.9	4.95	99.95
1	85.1	3.4	81.7
0.5	57.9	1	56.9

Bit error rate performance of terrestrial FSO link also depends on link length between transmitter and receiver since scintillation index (turbulence strength) is proportional to link length (section 2). FSO system should be designed to support as much link length as possible with good reliability and low power requirement. These criteria are fulfilled by ensuring reliable/satisfactory link operation in presence of strongest turbulence fading suffered by the system. According to the discussion of Section 2, this strongest turbulence fading will be characterized by the value of atmospheric refractive index structure parameter C_n^2. In [33], authors have experimentally found the maximum value of C_n^2 in a typical FSO link $2 * 10^{-13} m^{-2/3}$. Wavelength of transmitting laser beam is another important quantity for mitigation of scintillation induced fading. In current analysis it is chosen as 1.55 ¯m since this wavelength in the lowest atmospheric absorption region and because of its eye safety. Using these parametric values bit error rate performance of the system is evaluated in Figure 7 by varying link distance from 0.5 Km to 4 Km (since this distance is mostly used for practical FSO application).In this task, average CINR requirement is chosen as 10.2 dB which is actually found after some iteration. Performance of three systems such as un-coded BPSK without diversity, turbo coded ($N = 320$) 8-PSK without diversity and turbo coded 8-PSK with 4 photo detectors are illustrated. From this figure, error performance of all three systems got flattened after a certain distance to a particular bit error rate. The reason of saturation of BER versus. link length curve is the saturation of scintillation index after a particular link length. At this point controlling parameter of turbulence fading varies very slowly with distance and effect of scintillation fading almost seems to be unchanged with increase of link length. Scintillation induced fading is the only operating impairment for current analysis and no atmospheric attenuation as well as scattering effects is assumed to degrade system performance. For this reason after a particular distance (saturation length) BER gets floored instead of being increased. Main challenge is to maximize this saturation distance and minimize saturation BER. For last candidate of three systems it is possible to achieve a link length of 4 Km with a bit error rate 10^{-10} This result is interesting since for this link length turbulence strength goes to saturation region beyond strong regime with $\sigma_I^2 \approx 29$.

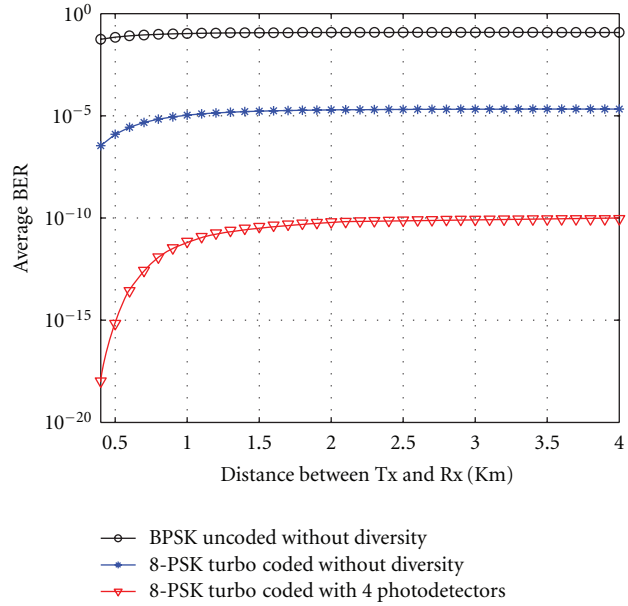

Figure 7: BER performance against achievable link length using 10.2 dB average CINR and 1.55 μm wavelength of laser beam in worst situation ($C_n^2 = 2 * 10^{-13} m^{-2/3}$).

From previous result, for ensuring good reliability minimum CINR requirement for proposed system is 10.2 dB. User allocation is another important issue since it is a multi-user system. This task is accomplished for the proposed system configuration with 256 chip GOLD sequence and 250 number of users. Average received optical power vs. CINR is profiled in Figure 8. From this figure 10.2 dB CINR is ensured when received optical power is −50.3 dBm. This is the minimum optical power requirement per photo detector for successful link operation with above user capacity.

Now proposed system provides an enhanced performance but definitely with more complexity than previous systems. To address complexity-performance trade-off issue following two parameters KPI (key performance indicator) and CPP (cost per performance) are introduced.

$$\text{KPI} = \frac{B * \text{S.I.}}{C}, \qquad \text{CPP} = \frac{N}{\text{KPI}}, \tag{30}$$

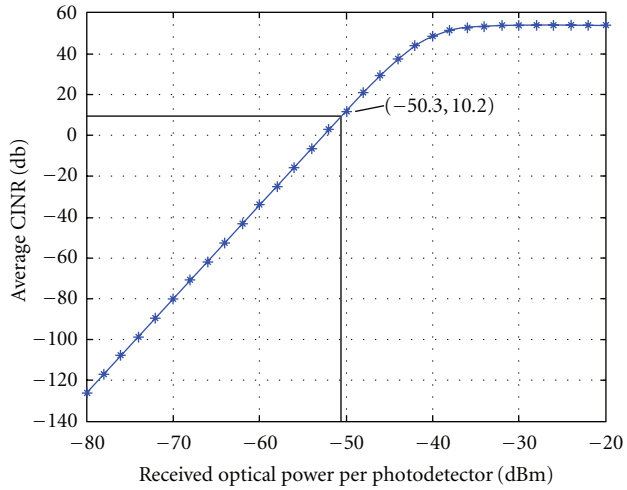

Figure 8: Received Optical Power vs. Average CINR using 8-PSK, Turbo Coded system with 4 Rx and 250 simultaneous user in strong turbulence fading.

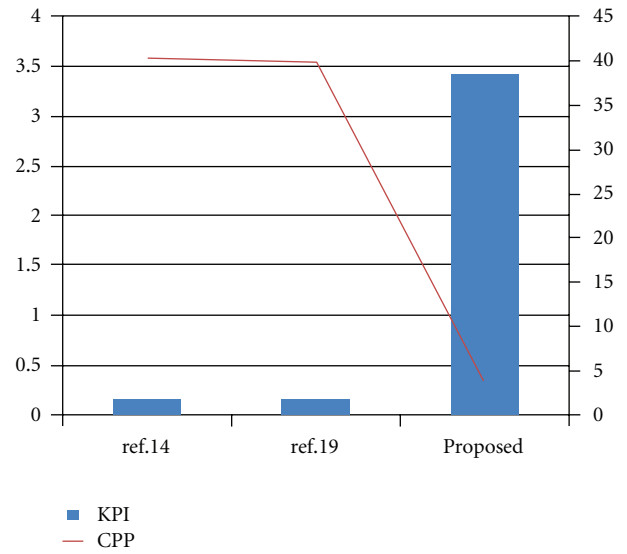

Figure 9: Complexity versus Performance Trade-off Comparison for Different FSO System.

where B = abs($\log_{10}$ (BER)), S.I. = Operating Scintillation Index, C = Minimum required CINR (in dB), and N = Number of required Components by system.

System design goal is to maximize KPI and minimize CPP. For present system number of required components, BER, minimum required CINR and operating scintillation index respectively 13 (from Figure 1), 10^{-10}, 10.2 dB and 3.5. For fair comparison with other systems single user supporting system is considered. Proposed system is compared with BPSK modulated, un-coded with 2 Rx (EGC) FSO system [19] and OOK modulated, un-coded with 3 Rx (maximal ratio combining) FSO system [14]. For former one above parameters are 7, 10^{-6}, 55 dB, 1.6 and for later one these parameters are 7, 10^{-8}, 57.5 dB and 1.25. Comparison of KPI and CPP of all three systems are illustrated in Figure 9.

Table 5: Proposed system profile in presence of strong turbulence fading.

Bit error rate	10^{-10}
Modulation/detection	8-ary PSK based subcarrier intensity modulation/direct detection
Number of photodetectors	4 (PIN photodetector)
Average electrical CINR per photodetector requirement	10.2 dB
Spreading sequence	256 chip GOLD sequence
Turbo-coding configuration	16 state Rate-1/3 (23, 37, 320) Turbo Code with $d_{\text{free}} = 23$ and $w_{\text{free}} = 1$
Laser beam wavelength	1.55 μm
Achievable link length	3 to 3.5 Km

It is clear from this figure that proposed system has much higher KPI than previous one whereas its CPP is much lower than previous one. It proves although system complexity is increased due to addition of some components because of integration of coding-higher order PSK mapping-diversity, still in terms of performance it is an optimum choice than previous competitors for cost efficiency. Availability of all such components is another issue and it should be noted all signal processing here are accomplished in RF domain rather than optical domain. In RF domain 8-PSK signal mapping is used in existing EDGE system and proposed turbo code configuration is used in 3G system. Consequently, components availability and implementation complexity is not a hindrance for successful operation of proposed system.

From simulation results, it is now possible to recommend a system profile for proposed system. This is shown in Table 5.

6. Conclusion

In this paper an analytical approach has been presented to improve the BER performance of MC-CDMA signal transmission over terrestrial FSO link through which the strong atmospheric turbulence induced fading is a strong limiting factor. By applying multi-level modulation, photo detector spatial diversity with equal gain combining and turbo coding with appropriate parameter, proposed system configuration displays a 10.2 dB average CINR requirement for operation over 4 Km link in strong turbulence fading condition with 10^{-10} BER and 250 number of user capacity. Additionally, performance enhancement-complexity trade-off for proposed system is also analyzed and system is shown to exhibit much lower cost per performance criteria than state of art systems.

Acknowledgment

The authors acknowledge to the support and assistance of EEE Department, BUET for completing this research work.

References

[1] D. Kedar and S. Arnon, "Urban optical wireless communication networks: the main challenges and possible solutions," *IEEE Communications Magazine*, vol. 42, no. 5, pp. S2–S7, 2004.

[2] H. H. Refai, J. J. Sluss, and H. H. Refai, "The transmission of multiple RF signals in free-space optics using wavelength division multiplexing," in *Atmospheric Propagation II*, vol. 5793 of *Proceedings of the SPIE*, pp. 136–143, Orlando, Fla, USA, March 2005.

[3] K. Kazaura, K. Wakamori, M. Matsumoto, T. Higashino, K. Tsukamoto, and S. Komaki, "RoFSO: a universal platform for convergence of fiber and free-space optical communication networks," *IEEE Communications Magazine*, vol. 48, no. 2, Article ID 5402676, pp. 130–137, 2010.

[4] G. Katz, S. Arnon, P. Goldgeier, Y. Hauptman, and N. Atias, "Cellular over optical wireless networks," *IEE Proceedings*, vol. 153, no. 4, pp. 195–198, 2006.

[5] A. Bekkali, P. T. Dat, K. Kazaura, K. Wakamori, and M. Matsumoto, "Performance analysis of SCM-FSO links for transmission of CDMA signals under gamma-gamma turbulent channel," in *Proceedings of the IEEE Military Communications Conference (MILCOM '09)*, pp. 1–5, Boston, Mass, USA, October 2009.

[6] B. Hamzeh and M. Kavehrad, "OCDMA-coded free-space optical links for wireless optical-mesh networks," *IEEE Transactions on Communications*, vol. 52, no. 12, pp. 2165–2174, 2004.

[7] T. A. Bhuiyan, M. D. Z. Hassan, S. M. S. Tanzil, S. Hayder, and S. P. Majumder, "Performance improvement of IM-DD free space optical CDMA (attenuated by strong atmospheric turbulence) with maximal ratio combining," in *Proceedings of the International Conference on Computational Intelligence and Communication Networks (CICN '10)*, pp. 513–518, Bhopal, Madhya Pradesh, India, 2010.

[8] T. A. Bhuiyan, S. H. Choudhury, A. Al-Rasheed, and S. P. Majumder, "Effect of atmospheric turbulence on free space optical Multi-Carrier Code Division Multiple Access(MC-OCDMA)," in *Proceedings of the 12th International Conference on Computer Modelling and Simulation (UKSim '10)*, pp. 553–557, London, UK, March 2010.

[9] S. S. Muhammad, T. Plank, E. Leitgeb et al., "Challenges in establishing free space optical communications between flying vehicles," in *Proceedings of the 6th International Symposium Communication Systems, Networks and Digital Signal Processing (CSNDSP '08)*, pp. 82–86, Graz, Austria, July 2008.

[10] H. Willebrand and B. S. Ghuman, *Free Space Optics: Enabling Optical Connectivity in Today's Network*, SAMS, Indianapolis, Ind, USA, 2002.

[11] J. C. Ricklin, S. M. Hammel, F. D. Eaton, and S. L. Lachinova, "Atmospheric channel effects on free-space laser communication," *Journal of Optical and Fiber Communications Research*, vol. 3, no. 2, pp. 111–158, 2006.

[12] B. Hamzeh and M. Kavehrad, *Characterization of Cloud Obscured Free Space Optical Channels*, U.S. Air Force Research Laboratory/Wright-Patterson, 2005.

[13] X. Zhu and J. M. Kahn, "Free-space optical communication through atmospheric turbulence channels," *IEEE Transactions on Communications*, vol. 50, no. 8, pp. 1293–1300, 2002.

[14] T. A. Tsiftsis, H. G. Sandalidis, G. K. Karagiannidis, and M. Uysal, "Optical wireless links with spatial diversity over strong atmospheric turbulence channels," *IEEE Transactions on Wireless Communications*, vol. 8, no. 2, pp. 951–957, 2009.

[15] Z. Hajjarian, J. Fadlullah, and M. Kavehrad, "MIMO free space optical communications in turbid and turbulent atmosphere (invited paper)," *Journal of Communications*, vol. 4, no. 8, pp. 524–532, 2009.

[16] F. Xu, A. Khalighi, P. Caussé, and S. Bourennane, "Channel coding and time-diversity for optical wireless links," *Optics Express*, vol. 17, no. 2, pp. 872–887, 2009.

[17] I. B. Djordjevic, B. Vasic, and M. A. Neifeld, "LDPC coded OFDM over the atmospheric turbulence channel," *Optics Express*, vol. 15, no. 10, pp. 6336–6350, 2007.

[18] W. O. Popoola, Z. Ghassemlooy, J. I. H. Allen, E. Leitgeb, and S. Gao, "Free-space optical communication employing subcarrier modulation and spatial diversity in atmospheric turbulence channel," *IET Optoelectronics*, vol. 2, no. 1, pp. 16–23, 2008.

[19] W. O. Popoola and Z. Ghassemlooy, "BPSK subcarrier intensity modulated free-space optical communications in atmospheric turbulence," *Journal of Lightwave Technology*, vol. 27, no. 8, pp. 967–973, 2009.

[20] W. O. Popoola and Z. Ghassemlooy, "Free-space optical communication in atmospheric turbulence using DPSK subcarrier modulation," in *Proceedings of the 9th International Symposium on Communication Theory and Application*, pp. 156–169, Ambleside, Lake District, UK, July 2007.

[21] M. A. Al-Habash, L. C. Andrews, and R. L. Phillips, "Mathematical model for the irradiance probability density function of a laser beam propagating through turbulent media," *Optical Engineering*, vol. 40, no. 8, pp. 1554–1562, 2001.

[22] S. M. Aghajanzadeh and M. Uysal, "Diversity–multiplexing trade-off in coherent free-space optical systems with multiple receivers," *Journal of Optical Communications and Networking*, vol. 2, no. 12, pp. 1087–1094, 2010.

[23] E. J. Lee and V. W. S. Chan, "Part 1: optical communication over the clear turbulent atmospheric channel using diversity," *IEEE Journal on Selected Areas in Communications*, vol. 22, no. 9, pp. 1896–1906, 2004.

[24] N. D. Chatzidiamantis, G. K. Karagiannidis, and D. S. Michalopoulos, "On the distribution of the sum of gamma-gamma variates and application in MIMO optical wireless systems," in *Proceedings of theIEEE Global Telecommunications Conference (GLOBECOM '09)*, pp. 1768–1773, Honolulu, Hawaii, USA, December 2009.

[25] J. G. Prokis, *Digital Communications*, McGraw–Hill Book Company, New York, NY, USA, 4th edition, 2001.

[26] M. Uysal, S. M. Navidpour, and J. Li, "Error rate performance of coded free-space optical links over strong turbulence channels," *IEEE Communications Letters*, vol. 8, no. 10, pp. 635–637, 2004.

[27] W. Gappmair and M. Flohberger, "Error performance of coded FSO links in turbulent atmosphere modeled by gamma-gamma distributions," *IEEE Transactions on Wireless Communications*, vol. 8, no. 5, pp. 2209–2213, 2009.

[28] W. E. Ryan, "Concatenated codes and iterative decoding," in *Willey Encyclopedia of Telecommunications*, G. Proakis, Ed., John Wiley & Sons, New York, NY, USA, 1st edition, 2003.

[29] N. Letzepis and A. Grant, "Bit error rate estimation for turbo decoding," in *Proceedings of the 4th Australian Communication Theory Workshop*, pp. 108–112, 2003.

[30] B. Vucetic and J. Yuan, *Turbo Codes: Principles and Applications*, Kluwer Academic Publishers, 2000.

[31] T. M. Duman and A. Ghrayeb, *Coding for MIMO Communication Systems*, chapter 7, John Wiley & Sons, New York, NY, USA, 2007.

[32] R. Garello, P. Pierleoni, and S. Benedetto, "Computing the free distance of turbo codes and serially concatenated codes with interleavers: algorithms and applications," *IEEE Journal on Selected Areas in Communications*, vol. 19, no. 5, pp. 800–812, 2001.

[33] K. Kazaura, T. Suzuki, T. Higashino et al., "Experimental demonstration of a radio on free space optics system for ubiquitous wireless," *PIERS Online*, vol. 5, no. 3, pp. 235–240, 2009.